Caldera collapse: Perspectives from comparing Galápagos volcanoes, nuclear-test sinks, sandbox models, and volcanoes on Mars

Keith A. Howard, *U.S. Geological Survey, 345 Middlefield Road, Menlo Park, California 94025-3591, USA, khoward@usgs.gov*

ABSTRACT

The 1968 trapdoor collapse (1.5 km^3) of Fernandina caldera in the Galapágos Islands developed the same kinds of structures as found in small sandbox-collapse models and in concentrically zoned sinks formed in desert alluvium by fault subsidence into underground nuclear-explosion cavities. Fernandina's collapse developed through shear failure in which the roof above the evacuating chamber was lowered mostly intact. This coherent subsidence contrasts to chaotic piecemeal collapse at small, rocky pit craters, underscoring the role of rock strength relative to subsidence size. The zoning at Fernandina implies that the deflated magma chamber underlay a central basin and a bordering inward-dipping monocline, which separates a blind inner reverse fault from an outer zone of normal faulting. Similar concentric zoning patterns can be recognized in coherent subsidence structures ranging over 16 orders of magnitude in size, from sandbox experiments to the giant Olympus Mons caldera on Mars.

INTRODUCTION

Calderas are ubiquitous features of many volcanic terrains, and field, numerical, and analog studies have generated numerous models of their collapse structure. This paper analyzes the structure of the largest well-documented historic caldera collapse to illustrate how comparisons to large and small scaled analogs shed light on the subsidence mechanics of structures in varied settings and over a huge size range. When the caldera floor of basaltic Volcán Fernandina in the Galápagos Islands subsided by 1.5 km^3 in 1968 (Simkin and Howard, 1970; Filson et al., 1973), it preserved structural details that can be compared directly to large, concentrically zoned sinks subsided into underground nuclear-explosion cavities, to laboratory sandbox models, and to other volcanic collapses.

The mechanical significance of caldera collapse structure has been apparent since Anderson's (1936, 1951) classic analyses of stress and faulting and his conclusion that outward-dipping faults would form above a deflating magma chamber, whereas inward-dipping fractures would form above an expanding chamber. Field studies have documented inward-dipping, outward-dipping, or vertical boundary faults at various calderas around the world (Lipman, 1997; Cole et al., 2005). Exposed caldera faults are limited, however, to mostly small vertical extents and the few exceptions where tilted calderas expose natural cross sections (John, 1995). Insightful mechanical models of caldera substructure have come from sandbox experiments in which material is withdrawn at depth (e.g. Roche et al., 2000). Such analogs were shown to mimic the 0.6 km^3 collapse in 2000 of Miyakejima caldera on both outward-dipping and inward-dipping faults (Geshi et al., 2002; Acocella, 2007).

The roof in most calderas is lowered mostly intact by shear failure along faults (Lipman, 1984, 1997). This describes a *coherent* style of subsidence, the style addressed in this paper, which characterizes large structures or weak collapse media so long as size and material strength scale together. These structures may vary in shape from saglike to pistonlike and from symmetrical to like a trapdoor. Coherent collapse contrasts with failure by chaotic piecemeal spalling, which characterizes most pit craters and other small collapses in rock that is strong relative to size. This underscores the influence of material strength relative to size on whether a collapse is piecemeal or coherent.

FERNANDINA CALDERA COLLAPSE, GALÁPAGOS

The well-preserved forms of Galápagos collapse calderas have prompted many studies and comparisons to other calderas on Earth and Mars. The 4 × 6.5-km-wide summit caldera of Fernandina was 700 m deep before the 1968 collapse, when it deepened another 350 m (Fig. 1; Simkin and Howard, 1970; Filson et al., 1973). Old benches at each end of the elliptical caldera exemplify earlier cycles of partial basalt filling and stranding by collapse, showing that, like many other basaltic calderas, Fernandina's has experienced repeated collapse and filling episodes (Peterson and Moore, 1987; Chadwick and Howard, 1991; Rowland and Munro, 1992; Mouginis-Mark and Rowland, 2001). Since 1968, many lava flows and a huge (1 km^3) 1988 landslide have accumulated ~200 m of caldera fill, hiding the collapse features (Chadwick et al., 1991; Allan and Simkin, 2000).

Before the 1968 collapse, Fernandina caldera's floor was 2.4 × 4.0 km across (Figs. 1 and 2). The floor was nearly flat except for a pre-1946 tuff cone 750 m wide and 130 m high. Large hydromagmatic eruptions vented from the caldera wall in early June 1968 (volcanic explosivity index [VEI] 4), likely triggered by groundwater flowing toward a lowering magma column, as is common when magma withdraws downward (Stearns and MacDonald, 1946; Hildreth, 1991; Dvorak, 1992). The volume of ash from that eruption and lava from an eruption on the volcano's flank three weeks earlier amounted to only a small percentage of the subsequent ~1.5 km^3 collapse (Simkin and Howard, 1970).

GSA Today, v. 20, no. 10, doi: 10.1130/GSATG82A.1

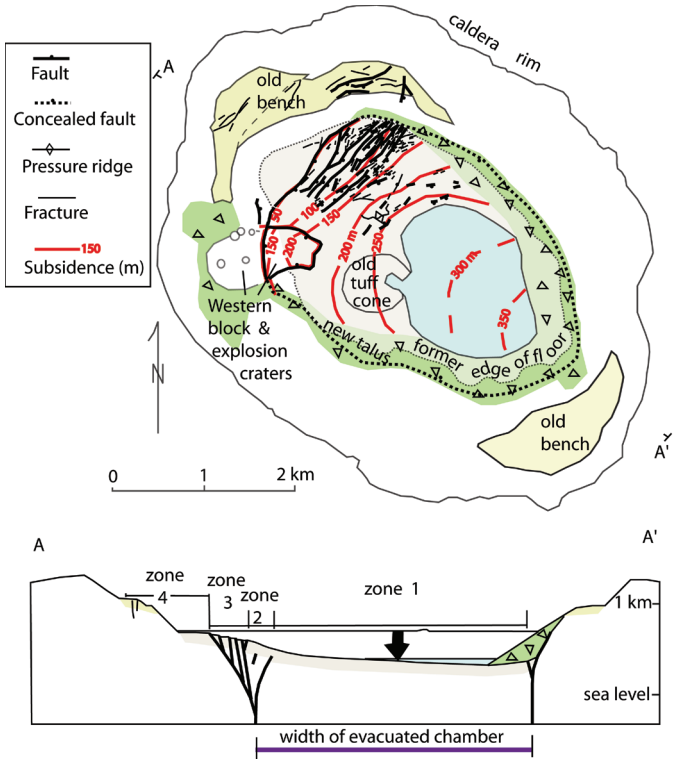

Figure 1. Sketch map of Fernandina caldera floor in July 1968 (central tinted area) showing new faults, subsidence contours, and new lake. Talus (green) covered much of the ring fault at the base of steep preexisting caldera walls. Interpretive cross section is based on resemblance of the collapsed floor to numbered zones in nuclear-test sinks and sandbox models. Faults are mapped from observations and photos in 1968 (Simkin and Howard, 1970), 1970, and 1971. Subsidence contours from pre-collapse and post-collapse photogrammetric mapping. Filson et al. (1973) reported lake depth, and mapped floor dips as steep as 30°. Location 0°22′S, 91°33′W.

A 10-day pulsating swarm of earthquakes (M_s 4 to 5.2) followed a day after the VEI-4 eruption and was modeled as ~75 incremental drops, ~5 m each, of a 2-km-wide piston as the floor subsided (Filson et al., 1973). The collapsed floor was faulted and strongly asymmetric, hinged trapdoor-like at one end and lowered 350 m at the other (Fig. 2). The preexisting tuff cone was tilted and lowered 250 m intact. A lake fed by groundwater during collapse drowned the most-lowered southeast end of the caldera floor. Avalanche debris derived from the south wall during the collapse draped part of the tuff cone and projected onto the submerged lake floor.

Subsidiary collapse dropped a smaller block at the western end of the caldera wall and floor, adjacent to the vent area for the hydromagmatic eruptions. The sunken western block accounted for <1% of the total collapse volume and likely relates to a cupola-like volume evacuated by ejected ash. The main floor collapse presumably resulted when magma vacated from under the caldera through withdrawal at depth, intrusion into another part of the edifice (Simkin and Howard, 1970), or venting out the submarine flank of the volcano (Geist et al., 2006; Glass et al., 2007). Caldera collapse commonly accompanies drainage to distant eruptions or intrusions (Sigardsson and Sparks, 1978; Nakada et al., 2005).

The edge of main collapse coincided mostly with the old edge of the caldera floor, where a talus-covered new fault can be inferred to coincide with a buried ring fault from previous collapse episodes. This coincidence in position suggests persistence of magma chamber position and possible influence by the preexisting faults and caldera shape.

The small, unfaulted northwest end of the caldera floor transitioned into the lowered part of the floor across a region of step faults and grabens. This faulted zone graded inward into an inward-dipping monocline, which bordered a broad inner basin.

SUBSIDENCE ANALOGS OVER NUCLEAR-TEST CAVITIES

Sink depressions formed by subsidence into deep, mostly spherical cavities made by underground nuclear explosions provide analogs much larger than sandbox models and intermediate in size to Fernandina and other volcanic calderas. Hundreds of these cavities formed at the Nevada Test Site eventually collapsed to the surface in desert alluvium, taking anywhere from minutes to years, and they were richly documented (Houser, 1969, 1970a, 1970b). The resulting sink depressions vary in steepness and size (6–500 m wide, 1–60 m

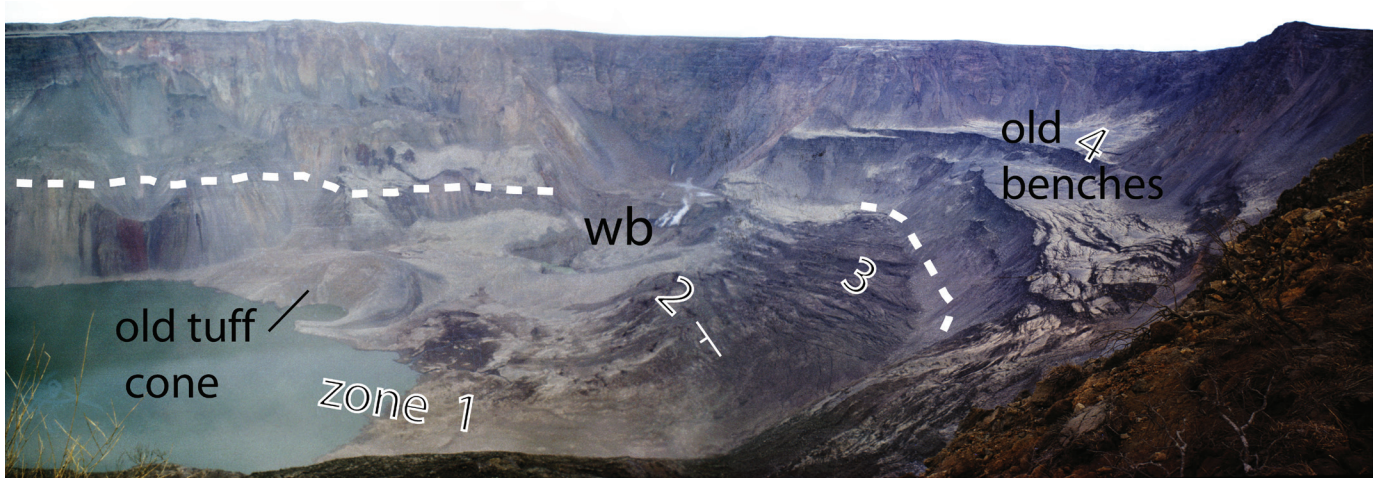

Figure 2. Fernandina caldera in July 1968, just after its floor collapsed from its former position (dashed line). View west shows sagged central floor (zone 1), monocline (zone 2), area of step faults and graben (3), and site of peripheral fractures (4) on old benches. Site of VEI-4 eruption is behind fuming western collapse block (wb).

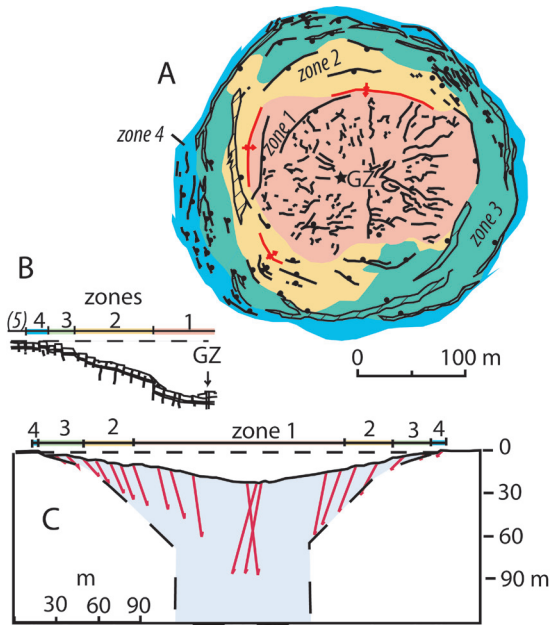

Figure 3. Structure of three typical sinks formed over buried nuclear-test cavities at Yucca Flat, Nevada, USA, from Houser (1969, 1970a). The shot cavities were centered below ground zero (GZ). (A) Map view of zones and faults in Aardvark sink. (B) Generalized morphologic zones in a sink; dashed line indicates original valley surface. Landslide debris coats a scarp boundary between zones 1 and 2. Zone 5 consists of outer fractures produced by the explosion and is unrelated to the subsequent collapse. (C) Representative surface displacements (red vectors exaggerated 4×) of the faulted subsided floor of a moderate-relief sink. Cross section of the deformed zone indicates cylindrical shape projected above the deeper shot cavity and the upward flaring inferred by Houser (1969), consistent with displacements toward a shallow focus.

deep); a typical sink may be 200 m wide and 20 m deep, and most have a faulted but intact floor (Fig. 3). The unique effects of the nuclear tests, namely the gas-filled, typically spherical explosion cavity and explosion-produced bulking and fracturing, appear to have relatively minor influence on the collapse geometry. Deeper nuclear-test cavities produced shallower and less voluminous collapse sinks in alluvium than did shallower nuclear-test cavities, even though the cavity depth did not much affect sink width (Houser, 1969). Some deep sinks did not collapse to the surface until years later, or not at all for the deepest ones (Houser, 1970a).

Collapse over the nuclear-test cavities proceeded toward the surface via a vertically elongating domed chimney until the topmost ~30 m dropped as a central plug. A peripheral near-surface zone then immediately collapsed inward, yielding a cross-sectional geometry that flares upward to a diameter at the surface about 2.5 times the cavity and chimney diameter (Fig. 3C). Points on the ground moved downward and inward toward a shallow focus consistent with the upward-flared near-surface structure.

Houser (1969) recognized four concentric structural-morphologic collapse zones at >90% of these sinks (Figs. 3A and 3B). The central, flat or saucer-shaped lowest part of a nuclear-test sink was designated zone 1. Ringing zone 1 and commonly separated from it by a fault scarp is zone 2, defined by a consistently inward tilt and showing the most inward displacement. Annular zone 3 is marked by concentric fault blocks that are subsided but not tilted and may include a bounding outer fault scarp. Fractured ground outside the area of major subsidence was designated zone 4. (A peripheral zone 5 of outer fracturing produced by the pre-collapse nuclear explosion is not important to the collapse.)

When a sink formed, the first surface expression was lowering of zone 1 overlying a central plug. This was followed immediately by widening and inward motion successively on zone 2 and then zone 3. Similar sequences were later documented at the collapse of Miyakejima caldera (Geshi et al., 2002) and in some sandbox caldera models (Roche et al., 2000; Kennedy et al., 2004). As the surface subsidence of a sink expanded outward, concentric fractures formed, and some then closed as successively outer zones moved centripetally inward and compressed the interior zones while outer zones distended (Houser, 1969). Zone 2 showed the greatest inward motion. Contractile pressure ridges formed in zones 1 and 2. The near-surface fault pattern in zones 2 and 3 could be highly complex in detail (Houser, 1970b), but the overall geometric and kinematic patterns of collapse were consistent among most sinks.

COMPARISON TO LABORATORY SANDBOX MODELS

Scale modeling of caldera collapse where support is withdrawn at depth in laboratory sandboxes has produced a consistent picture and sequence of coherent collapse (e.g., Roche et al., 2000; Acocella et al., 2000; Walter and Troll, 2001; Kennedy et al., 2004; Acocella, 2007; Martí et al., 2008). Commonly, these structures have been produced using material such as rough sand, wet sand, or sand mixed with a little powder to provide some cohesion as evidenced by the capability of sustaining small cliffs and faults (Fig. 4). The presence of faults, sags, and folds indicates failure primarily in compression and shear.

The surface in many sandbox caldera models mimics zones 1–4 at the nuclear-test sinks (Fig. 4). These experimental sandbox collapses begin with upward propagation of steep faults from the margins of a lowering or deflating magma-chamber analog, such as a buried bladder, balloon, piston, or dry ice (Roche et al., 2000; Acocella, 2007). Elegant laboratory sandbox structures reported by these and other research teams in the past decade can be imitated qualitatively in simple experiments. In some by the author in 1974, for example, deflation of a buried air balloon could be made to duplicate the surface morphology of nuclear-test sinks (Fig. 4). As a bell-shaped central block (zone 1) dropped along reverse faults, peripheral rings of material moved toward it, compressing it and helping to keep it intact while distending the outer zone-3 part of the structure and widening the structural diameter along normal faults, as at nuclear-test sinks.

Other features also simulated the sinks: the deformation field flared upward, funnel-like (Acocella, 2007); the models collapsed sequentially from depth to the surface and outward from the interior to the structural periphery; and increasing the chamber depth decreased the depth but not the width of surface subsidence (Roche et al., 2000). An inward-tilted zone 2 made up the hanging wall of the reverse-fault system. Size, shape, depth, and rate of evacuation of the modeled magma chamber influence details of the coherent sandbox collapse,

but overall deformation patterns found by several research teams using different experimental apparatus, shape, and properties of deflation chamber, as well as similarity analysis, remain strikingly consistent (e.g., Roche et al., 2000; Kennedy et al., 2004).

Collapses in laboratory media having too much cohesion relative to the size of structure produce analogs to pit craters rather than to coherent calderas (cf. Martí et al., 1994; Roche et al., 2001). For example, deflation of a small toy air balloon buried in dry powder generally will create vertical or overhanging pits floored by a pile of rubble resulting from tensile failure and piecemeal spalling. The spalled sandbox pits resemble hard-rock collapses smaller than calderas, including some mines and volcanic pit craters.

Similarity laws indicate that experimental analogs can scale kinematically to calderas in stronger media if physical properties such as size, strength, and stresses from weight scale proportionally (Hubbert, 1937; Michon and Merle, 2003). Fractured rocks in situ may have different strength properties than samples measured in the lab, so precise scaling from models to the larger structures is challenging. To semi-quantitatively test scaling of models that fail in shear, the height of maximum fault scarp can be a good proxy for strength. This is because the critical maximum height (Hcr) of a vertical cliff that the material can support provides a useful approximation of relative cohesive strength (Tschebotarioff, 1951). Roche et al. (2001) also used this relation. Similar ratios of structural width (D) to cliff height for morphologically similar sandbox collapse models (D:Hcr = 3 to 12), nuclear-test sinks (D:Hcr = 8 to 25), and Fernandina caldera (D:Hcr = 7 to 8) are consistent with geometric and mechanical similarities among them[1].

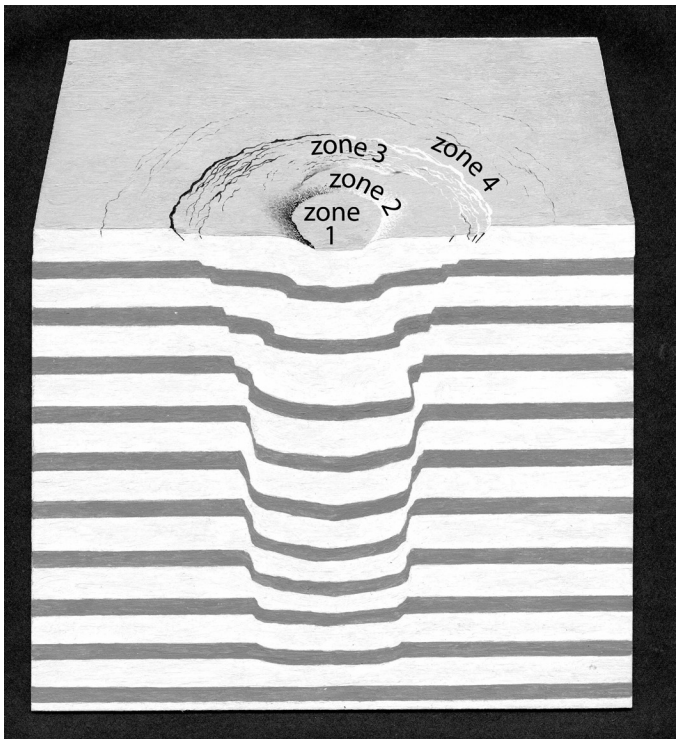

Figure 4. Artist's illustration of sandbox-model deformation caused by deflating an air balloon 6.5 cm across and 4.5 cm high buried under colored layers behind a plastic window. Layers were a mix of five parts sand to one part plaster of Paris powder. The pre-inflated balloon was flattened by the weight above it. As the balloon was deflated, faults propagated upward, dropping a central plug (zone 1) between reverse faults or monoclines (zone 2), followed by inward movement along peripheral normal faults in zone 3. (The balloon withdrew back from the window as it deflated.) The surface morphology mimicked similar experiments centered in the sandbox, showing that window friction had little effect. Collapse geometry was insensitive to deflation speed. A second set of reverse faults sometimes developed (see also Martí et al., 1994; Roche et al., 2000). Painted by Don Davis in 1974, idealized slightly from imperfectly parallel initial layering in sandbox experiments performed under the author's direction.

INTERPRETATION OF FERNANDINA COLLAPSE

The shape and structures of Fernandina's 1968 collapsed floor compare well, despite the collapse asymmetry, with the concentric zoning at nuclear-test sinks and coherent sandbox models. Cliffs as high as 300–500 m in Fernandina and Volcán Wolf calderas establish the Hcr and relative strength of Galápagos basalt, and similar ratios of Hcr to collapse diameter suggest kinematic and dynamic similarity to the sinks and sandbox models (see footnote 1). The typical zones are identifiable at Fernandina as the broad inner sag (zone 1), monocline (zone 2), step faults and grabens (zone 3), and peripheral cracks (zone 4) (Figs. 1 and 2). Analogy to sandbox models suggests that a blind reverse fault underlies the zone-2 monocline at Fernandina and bounds it against the central plug. Experience from the models suggests that greater surface faulting would have resulted if collapse had been deeper, as it was at Miyakejima caldera (Acocella, 2007; Geshi, 2009).

The lowered block was likely about as thick as it was wide, because magma chambers underlying Galápagos summit calderas typically are modeled as flat-topped and at depths of ~2 km (e.g., Chadwick and Dieterich, 1995; Geist et al., 2005; Yun et al., 2006). A width to thickness ratio of ~1 is consistent with the highly faulted zone 3, akin to sandbox collapses of thin roofs in which the normal faults are better developed than for thicker roofs (Roche et al., 2000). Lack of an outcropping reverse fault at the boundary between zones 1 and 2 in Fernandina is more akin to relatively thicker roofs in sandbox analogs (Roche et al., 2000).

A trapdoor asymmetry as at Fernandina's collapsed floor is also seen at many other calderas (Lipman, 1984), a nuclear-test site (Crowley et al., 1971), and in some sandbox models (Roche et al., 2000; Acocella et al., 2000; Kennedy et al., 2004). Trapdoor model geometries resulted from small heterogeneities in the models or from a variety of differences in chamber tilt or shape (Acocella, 2007).

Comparison of Fernandina's collapsed floor to the analogs implies that the subsided block at depth and the deflated chamber underlay zones 1 and 2 (Fig. 1). Magma chambers in basaltic shields commonly are thought to consist in detail of a network of small, interconnected chambers (Fiske and Kinoshita, 1969). If

[1] GSA supplemental data item 2010265, typical dimensions and densities for coherent experimental sandbox collapses, nuclear-test sinks in desert alluvium, Fernandina caldera in basalt, and calderas on Mars, is available online at www.geosociety.org/pubs/ft2010.htm. You can also request a copy from *GSA Today*, P.O. Box 9140, Boulder, CO 80301, USA; gsatoday@geosociety.org.

the Galápagos chambers are like this, interconnected magma flow must be unimpeded enough to allow rapid, large-volume lateral drainage ≥1.5 km^3, because the rapidity and steady rate of seismic energy release of Fernandina's 1968 collapse (Filson et al., 1973; Michon et al., 2009) suggest that magma migrated from beneath the caldera at a rate exceeding 0.1 km^3/day.

Basaltic chamber systems typically only partly drain; chamber volumes estimated for Kilauea, Hawaii, USA, for example, range from 2 to 240 km^3, much larger than recorded subsidence or eruptive volumes there (Johnson, 1992; Denlinger, 1997). Fernandina and the two other deepest Galápagos calderas, at Volcáns Wolf and Cerro Azul, all lie on the western edge of the Galápagos submarine platform where the unbuttressed flanks (Geist et al., 2006, 2008) may allow submarine eruptions occasionally to drain large thicknesses from the magma chambers.

OTHER CALDERAS

Post-collapse lava flows obscure floor collapse shapes in most other Galápagos calderas, except for the Bahia Darwin caldera that indents the low Genovesa Island volcano (0°19′S, 89°57′W). Physiographic analysis suggests that the 2-km-wide circular bay (bahia) is floored by a zone 1 that subsided 260 m and by a narrow submerged zone-2 slope; a 1-km-wide array of exposed concentric normal faults that rings the bay (Harpp et al., 2002) is subsided 30–60 m and is zone 3. This collapse structure, unlike Fernandina's, does not follow any preexisting caldera faults.

The caldera floor structures observed at Fernandina, Bahia Darwin, and Miyakejima are all on basaltic volcanoes, but some volcanic calderas of a wide compositional range show inward-tilted and sagged beds (zone 2) below the (commonly buried) collapsed floor. Outward-dipping ring faults comparable to the zone 1–2 reverse-fault boundary are detected seismically at some moderate-sized calderas (Mori and McKee, 1987; Nettles and Ekström, 1998).

The caldera of Olympus Mons (Fig. 5) and other giant calderas on Martian shield volcanoes also show the familiar structural zoning (Branney, 1995). The oldest and widest (65 km) of several intersecting, nested parts of the Olympus Mons caldera exhibits a fault-distended zone 3 with outer scarp and a zone-2 monocline with mapped concentric pressure ridges (Mouginis-Mark and Robinson, 1992; Zuber and Mouginis-Mark, 1992). Younger lava flows flood the inferred zone 1 and some other nested collapses. Other martian calderas, such as on Ascraeus Mons (40 km wide) and Arsia Mons (120 km wide), contain fault zones classifiable as zones 4, 3, or 2, partly concealed by younger infilling flows. The calderas on Mars formed under a gravitational field only 38% of Earth's and exhibit scarps up to 3–4 km high (see footnote 1), so they would model correspondingly smaller terrestrial analogs, but they are still huge collapses, 16 orders of magnitude larger in volume than sandbox analogs. The similarities imply that the large Martian calderas collapsed upon deflation of very broad magma chambers and behaved mechanically much like Fernandina, Miyakejima, and the nuclear-test and sandbox analogs.

DISCUSSION

The consistent structural zoning in collapse structures varying from symmetric to Fernandina's trapdoor floor suggests

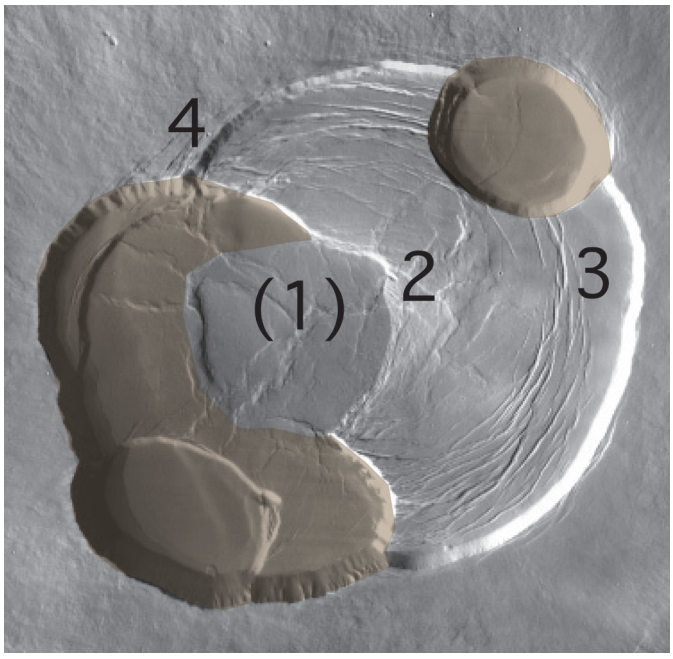

Figure 5. Olympus Mons caldera, Mars, 3–4 km deep (THEMUS image). The widest (65 km) and oldest part of the caldera (gray; crater 1 of Mouginis-Mark and Robinson, 1992; younger nested structures are shown tinted) shows the characteristic zoning. The zones are peripheral fractures (zone 4); a faulted zone 3, including bounding fault scarp; and a monocline, zone 2, in which Mouginis-Mark and Robinson (1992) mapped numerous concentric pressure ridges. A central plug, zone 1, is inferred to underlie younger, bowl-shaped and pressure-ridged lava fill.

analogous underlying fault geometries and mechanisms. Caldera types ranging from downsags to pistonlike also may be variations on a common mechanism, depending mainly on degree of collapse (Acocella, 2007). This idea is consistent with the gradation of Fernandina's floor from hinged at one end to deeply lowered, more like a piston, at the other.

Geometric and mechanical similarities of collapse structures ranging in volume over 16 orders of magnitude (see footnote 1) imply that, despite complexities in the natural systems, many basaltic calderas over a large size range may founder by similar fault mechanisms and geometries.

The structural collapse details observed on Fernandina's floor are now buried. A wide variety of other calderas, although also obscured, show at least some features that suggest structural similarity to the sandbox analogs (Acocella, 2007). Some catastrophically collapsed silicic ash-flow calderas are included, even though other factors, such as magma stirring (Kennedy et al., 2008) or fluidized material surging up ring fractures, might be expected to influence their collapse.

Inward tilting or folding in zone 2 reflects both the inward and downward displacement and also the convex-upward geometry of the exterior bounding faults (Fig. 4). In contrast to the back-tilting that occurs on listric, concave-upward faults, downsliding on convex-upward caldera boundaries naturally tends to tilt rocks inward (but not necessarily by fault drag; cf. Branney, 1995). Inward tilt typically results where vertical support is withdrawn, as in calderas, whereas backward tilt often results from loss of lateral support, as in landslide Toreva

blocks, slumped walls of impact craters (Howard, 1975) and some calderas (e.g., Ascraeus Mons), and tectonically extended terrains (Hamblin, 1965).

The inner contraction and peripheral extension from centripetal inward displacement during sandbox and nuclear-test subsidence is also seen at lava-lake crusts, some large volcanic pit craters, and in subsidence caused by mining and by fluid extraction (Swanson and Peterson, 1972; Castle and Yerkes, 1976; Branney, 1995; Rymer et al., 1998; Odonne et al., 1999). Ice-melt collapse pits and subsidence structures caused by dissolution can also show the familiar structural zoning (Branney and Gilbert, 1995; Maione, 2001).

It has been a common perception that doming would be required to solve a supposed caldera room problem: Like a cork in a bottle, downward-tapered collapse couldn't proceed unless a volcano first swells. Although inflation may precede and influence some caldera collapses, analog modeling shows that tumescence is not a prerequisite, nor are preexisting faults. Characteristic reverse in addition to normal faulting, and the weakness of earth materials compared to gravitational forces, explain how deflation can be sufficient cause for collapse.

CONCLUSIONS

Structural-morphologic zoning identified at the nuclear-test sinks in desert alluvium guides a way to link analogs and many volcanic collapse structures. Despite limitations of the sandbox and nuclear-test analogs for modeling complex volcanic systems, structural consistency and similarity analysis reinforce the usefulness of such analogs for interpreting caldera collapse. The structural comparisons help guide analysis of kinematics, reverse and normal faulting, and shape of the deflated chamber at volcanic collapses varying in size, shape, setting, and symmetry. That similar structural zoning is identifiable over 16 orders of volume magnitude up to giant Martian calderas suggests that similar geometries and mechanics can apply to many calderas.

ACKNOWLEDGMENTS

Tom Simkin (1933–2009) led our initial collaborative field work. Mitch Kingery and John Nakata helped construct sandbox models in 1974, and Don Davis illustrated them. Ray Jordan prepared pre-collapse and post-collapse photogrammetric maps of Fernandina. Fred Houser and Mike Carr also helped me. Steve Sparks, Steve Self, and others commented helpfully on my 1970s and 1980s presentations in Honolulu, Santiago, Hilo, Washington, and Cambridge comparing the sandbox and nuclear-test analogs to calderas. This paper was improved thanks to thoughtful critiques by William Chadwick, Peter Lipman, David Fastovsky, Bob Christiansen, Paul Stone, and two anonymous reviewers.

REFERENCES CITED

Acocella, V., 2007, Understanding caldera structure and development; an overview of analog models compared to natural calderas: Earth-Science Reviews, v. 85, p. 125–160.

Acocella, V., Cifelli, F., and Funiciello, R., 2000, Analogue models of collapse calderas and resurgent domes: Journal of Volcanology and Geothermal Research, v. 10, p. 81–96.

Allan, J.F., and Simkin, T., 2000, Fernandina Volcano's evolved, well-mixed basalts; mineralogical and petrological constraints on the nature of the Galapagos plume: Journal of Geophysical Research, v. 105, B3, p. 6017–6041.

Anderson, E.M., 1936, The dynamics of the formation of cone sheets, ring dykes, and cauldron subsidence: Royal Society of Edinburgh Proceedings, v. 56, part 2, p. 128–163.

Anderson, E.M., 1951, The dynamics of faulting and dyke formation with applications in Britain, second edition: London, Oliver and Boyd, 206 p.

Branney, M.J., 1995, Downsag and extension at calderas; new perspectives on collapse geometries from ice-melt, mining, and volcanic subsidence: Bulletin of Volcanology, v. 57, p. 303–318.

Branney, M.J., and Gilbert, J.S., 1995, Ice-melt collapse pits and associated features in the 1991 lahar deposits of Volcan Hudson, Chile; criteria to distinguish eruption-induced glacier melt: Bulletin of Volcanology, v. 57, p. 293–302.

Castle, R.O., and Yerkes, R.F., 1976, Recent surface movements in the Baldwin Hills, Los Angeles County, California: U.S. Geological Survey Professional Paper 882, 125 p.

Chadwick, W.W., and Dieterich, J.H., 1995, Mechanical modeling of circumferential and radial dike intrusion on Galápagos volcanoes: Journal of Volcanology and Geothermal Research, v. 66, p. 37–52.

Chadwick, W.W., and Howard, K.A., 1991, The pattern of circumferential and radial eruptive fissures on the volcanoes of Fernandina and Isabela Islands, Galápagos: Bulletin of Volcanology, v. 53, p. 259–275.

Chadwick, W.W., De Roy, T., and Carrasco, A., 1991, The September 1988 intracaldera avalanche and eruption at Fernandina volcano, Galápagos Islands: Bulletin of Volcanology, v. 53, p. 276–286.

Cole, J.W., Nilner, D.M., and Spudis, K.D., 2005, Calderas and caldera structures; a review: Earth Science Reviews, v. 69, p. 1–26.

Crowley, B.K., Glenn, H.D., and Marks, R.E., 1971, An analysis of Marvel—a nuclear shock-tube experiment: Journal of Geophysical Research, v. 76, p. 3356–3374.

Denlinger, R.P., 1997, A dynamic balance between magma supply and eruption rate at Kilauea volcano, Hawaii: Journal of Geophysical Research, v. 102, B8, p. 18,091–18,100.

Dvorak, J.J., 1992, Mechanism of explosive eruptions of Kilauea volcano, Hawaii: Bulletin of Volcanology, v. 54, p. 638–645.

Filson, J., Simkin, T., and Leu, L.K., 1973, Seismicity of a caldera collapse, Galápagos Islands 1968: Journal of Geophysical Research, v. 78, p. 8591–8622.

Fiske, R.S., and Kinoshita, W.T., 1969, Inflation of Kilauea volcano prior to its 1967–1968 eruption: Science, v. 165, p. 341–349.

Geist, D.J., Naumann, T.R., Standish, J.J., Kurz, M.D., Harpp, K.S., White, W.M., and Fornari, D.J., 2005, Wolf volcano, Galápagos archipelago; melting and magmatic evolution at the margins of a mantle plume: Journal of Petrology, v. 46, p. 2197–2224, doi:10.1093/petrology/egi052.

Geist, D.J., Fornari, D.J., Kurz, M.D., Harpp, K.S., Soule, S.A., Perfit, M.R., and Koleszar, A.M., 2006, Submarine Fernandina; Magmatism at the leading edge of the Galápagos hot spot: Geochemistry Geophysics Geosystems, v. 7, Q12007, 27 p., doi:10.1029/2006GC001290.

Geist, D.J., Diefenbach, B.A., Fornari, D.J., Kurz, M.D., Harpp, K.S., and Blusztajn, J., 2008, Construction of the Galápagos platform by large submarine volcanic terraces: Geochemistry Geophysics Geosystems, v. 9, no. 3, Q03015, doi:10.1029/2007GC001795.

Geshi, N., 2009, Asymmetric growth of collapsed caldera by oblique subsidence during the 2000 eruption of Miyakejima, Japan: Earth and Planetary Science Letters, v. 280, p. 149–158, doi:10.1016/j.epsl.2009.01.027

Geshi, N., Shimano, T., Chiba, T., and Nakada, S., 2002, Caldera collapse during the 2000 eruption of Miyakejima volcano, Japan: Bulletin of Volcanology, v. 64, p. 55–68.

Glass, J.B., Fornari, D.J., Hall, H.F., Cougan, A.A., Berkenbosch, H.A., Holmes, M.L., White, S.M., and de la Torre, G., 2007, Submarine volcanic morphology of the western Galápagos based on EM300 bathymetry and MR1 side-scan sonar: Geochemistry Geophysics Geosystems, v. 8, no. 3, doi:10.1029/2006GC001464.

Hamblin, K., 1965, Origin of "reverse drag" on the downthrown side of normal faults: Geological Society of America Bulletin, v. 76, p. 2231–2251.

Harpp, K.S., Wirth, K.R., and Korich, D.J., 2002, Northern Galapagos Province; hotspot-induced, near-ridge volcanism at Genovesa Island: Geology, v. 30, p. 399–402.

Hildreth, W., 1991, The timing of caldera collapse at Mount Katmai in response to magma withdrawal toward Norarupta: Geophysical Research Letters, v. 18, p. 1541–1544.

Houser, F.N., 1969, Subsidence related to underground nuclear explosions, Nevada Test site: Seismological Society of America Bulletin, v. 59, p. 2233–2251.

Houser, F.N., 1970a, A summary of information and ideas regarding sinks and collapse, Nevada Test Site: U.S. Geological Survey Report USGS-474-41 (NTS-216), 129 p.

Houser, F.N., 1970b, Near-surface sink structure, Nevada Test Site: U.S. Geological Survey Report USGS-474-36 (NTS-217), 30 p.

Howard, K.A., 1975, Geologic map of the crater Copernicus: U.S. Geological Survey Miscellaneous Geological Investigations Map I-840; scale: 1:250,000.

Hubbert, M.K., 1937, Theory of scale models as applied to the study of geologic structures: Geological Society of America Bulletin, v. 48, p. 1459–1519.

John, D.A., 1995, Tilted middle Tertiary ash-flow calderas and subjacent granitic plutons, southern Stillwater Range, Nevada; cross sections of an Oligocene igneous center: Geological Society of America Bulletin, v. 107, p. 180–200, doi: 10.1130/00167606(1995)107<0180:TMTAFC>2.3.CO;2.

Johnson, D.J., 1992, Dynamics of magma storage in the summit reservoir of Kilauea volcano, Hawaii: Journal of Geophysical Research, v. 97, B2, p. 1807–1820.

Kennedy, B., Stix, J., Vallance, J.W., Lavallée, Y., and Longpre, M-A., 2004, Controls on caldera structure; results from analog sandbox modeling: Geological Society of America Bulletin, v. 116, p. 515–524.

Kennedy, B.M., Jellinek, A.M., and Stix, J., 2008, Coupled caldera subsidence and stirring inferred from analogue models: Nature Geoscience, v. 1, p. 385–389.

Lipman, P.W., 1984, The roots of ash-flow calderas in western North America; windows into the tops of granitic batholiths: Journal of Geophysical Research, v. 89, p. 8801–8841.

Lipman, P.W., 1997, Subsidence of ash-flow calderas; relation to caldera size and magma-chamber geometry: Bulletin of Volcanology, v. 59, p. 198–218.

Maione, S.J., 2001, Discovery of ring faults associated with salt withdrawal basins, Early Cretaceous age, in the East Texas Basin: The Leading Edge, v. 20, p. 818–829, doi: 10.1190/1.1487290.

Martí, J., Ablay, G.J., Redshaw, L.T., and Sparks, R.S.J., 1994, Experimental studies of collapse calderas: Journal of the Geological Society, v. 151, p. 919–929.

Martí, J., Geyer, A., Folch, A., and Gottsmann, J., 2008, A review on collapse caldera modeling, *in* Gottsmann, J., and Martí, J., eds., Caldera volcanism; analysis, modelling, and response: Developments in Volcanology, v. 10, p. 233–283.

Michon, L., and Merle, O., 2003, Mode of lithospheric extension; conceptional models from analogue modeling: Tectonics, v. 22, 1028, 15 p., doi: 10.1029/2002TC001435.

Michon, L., Villeneuve, N., Catry, T., and Merle, O., 2009, How summit calderas collapse on basaltic volcanoes; new insights from the April 2007 caldera collapse of Piton de la Fournaise volcano: Journal of Volcanology and Geothermal Research, v. 184, p. 138–151, doi:10.1016/j.jvolgeores.2008.11.003.

Mori, J., and McKee, C., 1987, Outward-dipping ring-fault structure at Rabaul caldera as shown by earthquake locations: Science, v. 235, p. 193–195.

Mouginis-Mark, P.J., and Robinson, M.S., 1992, Evolution of the Olympus Mons caldera, Mars: Bulletin of Volcanology, v. 54, p. 347–360.

Mouginis-Mark, P.J., and Rowland, S.K., 2001, The geomorphology of planetary calderas: Geomorphology, v. 37, p. 201–223.

Nakada, S., Nagai, M., Kaneko, T., Nozawa, A., and Suzuki-Kamata, K., 2005, Chronology and products of the 2000 eruption of Miyakejima Volcano: Bulletin of Volcanology, v. 67, p. 205–218.

Nettles, M., and Ekström, G., 1998, Faulting mechanism of anomalous earthquakes near Bardarbunga volcano, Iceland: Journal of Geophysical Research, v. 103, p. 17,973–17,983.

Odonne, F., Menard, I., Massonnat, G.J., and Rolando, J-P., 1999, Abnormal reverse faulting above a depleting reservoir: Geology, v. 27, p. 111–114.

Peterson, D.W., and Moore, R.B., 1987, Geologic history and evolution of geologic concepts, island of Hawaii, *in* Decker, R.W., Wright, T.L, and Stauffer, P.H., eds., Volcanism in Hawaii: U.S. Geological Survey Professional Paper 1350, p. 149–189.

Roche, O., Druitt, T.H., and Merle, O., 2000, Experimental study of caldera formation: Journal of Geophysical Research, v. 105, B1, p. 395–416.

Roche, O., VanWyk de Vries, B., and Druitt, T.H., 2001, Sub-surface structures and collapse mechanisms of summit pit craters: Journal of Volcanology and Geothermal Research, v. 105, p. 1–18.

Rowland, S.K., and Munro, D.C., 1992, The caldera of Volcán Fernandina; a remote sensing study of its structure and recent activity: Bulletin of Volcanology, v. 55, p. 97–109.

Rymer, H., van Wyk de Vries, B., and Stix, J., 1998, Pit crater structure and processes governing persistent activity at Masaya volcano, Nicaragua: Bulletin of Volcanology, v. 59, p. 345–355.

Sigardsson, H., and Sparks, R.S.J., 1978, Lateral magma flow within rifted Icelandic crust: Nature, v. 274, p. 126–130.

Simkin, T., and Howard, K.A., 1970, Caldera collapse in the Galápagos Islands, 1968: Science, v. 169, no. 3944, p. 429–437.

Stearns, H.T., and MacDonald, G.A., 1946, Geology and ground-water resources of the island of Hawaii: Hawaii Division of Hydrography Bulletin 9, 363 p.

Swanson, D.A., and Peterson, D.W., 1972, Partial draining and crustal subsidence of Alae lava lake, Kilauea volcano, Hawaii: U.S. Geological Survey Professional Paper 800C, p. C1–C14.

Tschebotarioff, G.P., 1951, Soil Mechanics, Foundations, and Earth Structures: New York, McGraw-Hill Book Co. Inc., 645 p.

Walter, T.R., and Troll, V.R., 2001, Formation of caldera periphery faults; an experimental study: Bulletin of Volcanology, v. 63, p. 191–203.

Yun, S., Segall, P., and Zebker, H., 2006, Constraints on magma chamber geometry at Sierra Negra volcano, Galápagos Islands, based on InSAR observations: Journal of Volcanology and Geothermal Research, v. 150, p. 232–243.

Zuber, M.T., and Mouginis-Mark, P.J., 1992, Caldera subsidence and magma chamber depth of the Olympus Mons volcano: Journal of Geophysical Research, v. 97, E11, p. 18,295–18,307.

Manuscript received 29 Sept. 2009; accepted 18 Feb. 2010.